Journal of Molecular Graphics and Modelling 38 (2012) 165–173

Contents lists available at SciVerse ScienceDirect

Journal of Molecular Graphics and Modelling

journal homepage: www.elsevier.com/locate/JMGM

Investigation of a predicted N-terminal amphipathic α-helix using atomistic molecular dynamics simulation of a complete prototype poliovirus virion

Jason A. Roberts[a,b,*], Michael J. Kuiper[c], Bruce R. Thorley[a,b], Peter M. Smooker[b], Andrew Hung[b]

[a] World Health Organization Poliomyelitis Regional Reference Laboratory, Victorian Infectious Diseases Reference Laboratory, North Melbourne, Australia
[b] School of Applied Sciences and Health Innovations Research Institute, RMIT University, Melbourne, Australia
[c] Victorian Life Sciences Computation Initiative, Parkville, Australia

ARTICLE INFO

Article history:
Accepted 22 June 2012
Available online 6 July 2012

Keywords:
Molecular dynamics
Poliovirus
Enterovirus
Virus
Simulation
Structural virology

ABSTRACT

The wild type 1 poliovirus capsid was first described in atomic detail in 1985 using X-ray crystallography. Numerous poliovirus capsid structures have been produced since, but none resolved the spatial positioning and conformation of a predicted N-terminal α-helix of the capsid protein VP1, which is considered critical to virus replication. We studied the helical structure under varying conditions using *in silico* reconstruction and atomistic molecular dynamics (MD) simulation methods based on the available poliovirus capsid atom coordinate data. MD simulations were performed on the detached N-terminal VP1 helix, the biologically active pentamer form of the pre-virion structure, reconstructed empty virus capsids and a full virion containing the poliovirus RNA genome in the form of a supercoiled structure. The N-terminal α-helix structure proved to be stable and amphipathic under all conditions studied. We propose that a combination of spatial disorder and proximity to the genomic RNA made this particular structure difficult to resolve by X-ray crystallography. Given the similarity of our *in silico* model of poliovirus compared to X-ray crystallography data, we consider computational methods to be a useful complement to the study of picornaviruses and other viruses that exhibit icosahedral symmetry.

1. Background

Poliovirus is classified within the enterovirus genus of the family *Picornaviridae* which includes more than 90 human enteroviruses [1]. The single stranded positive sense RNA genome is enclosed by a non-enveloped capsid composed of 60 copies of four viral proteins: VP1, VP2, VP3 and VP4 (Fig. 1). One copy of each VP protein forms a protomer subunit and five individual protomers form a pentamer structure. The complete capsid has an icosahedral formation made from 12 pentamers. Integral to the capsid structure are myristate molecules covalently bound to the N-terminus of VP4 and an endogenous lipid occupying a hydrophobic pocket accessible from the exterior surface of VP1 that is common to enteroviruses. The RNA genome is polyadenylated and VPg, a virus encoded protein, is covalently attached to the 5′ terminus.

The wild poliovirus type 1 (Mahoney strain) capsid structure was resolved to 2.9 Å resolution by X-ray crystallography in 1985 [2]. However, certain regions could not be resolved from the electron density maps: residues 1–20 of the N-terminus of VP1, residues 1–7 of the N-terminus of VP2, residues 234–238 of the C-terminus of VP3 and residues 1–12 of the N-terminus of VP4. The N-termini of VP1, VP2 and VP4 are each located on the inner surface of the virion and it was postulated that they could not be resolved by X-ray crystallography due to spatial orientation compared to the symmetric icosahedral structure [2]. Prior to assembly into the final capsid structure, biologically active proteins in the form of pentamers are present, comprising five protomers with VP1, VP3 and a precursor protein VP0, which is cleaved during the assembly of infectious 160S particles to form VP2 and VP4. This process is hypothesised to involve cleavage of a scissile bond in the presence of RNA, essentially locking the capsid in its final and infectious conformation [3].

Since the initial atomic description of the poliovirus capsid in 1985, more than twenty coordinate files of poliovirus 1, 2 and 3 capsid structures have been submitted to the Worldwide Protein Data Bank and include complete virus and empty capsid structures. However, the N-terminus of VP1 was not resolved by any of these investigations. This may have been due to spatial disorientation or molecular movement of the protein chain. Proximity to the RNA core within complete virus particles may also have rendered the polypeptide unresolvable by X-ray crystallography although this was considered not to be a contributing factor when the first crystal structure was published in 1985 [4]. The amino

* Corresponding author at: National Enterovirus Reference Laboratory, WHO Poliomyelitis Regional Reference Laboratory, Victorian Infectious Diseases Reference Laboratory, 10 Wreckyn Street, North Melbourne 3051, Australia.
Tel.: +61 3 9342 2607; fax: +61 3 9342 2665.
E-mail address: jason.roberts@mh.org.au (J.A. Roberts).

1093-3263/$ – see front matter © 2012 Elsevier Inc. All rights reserved.
http://dx.doi.org/10.1016/j.jmgm.2012.06.009

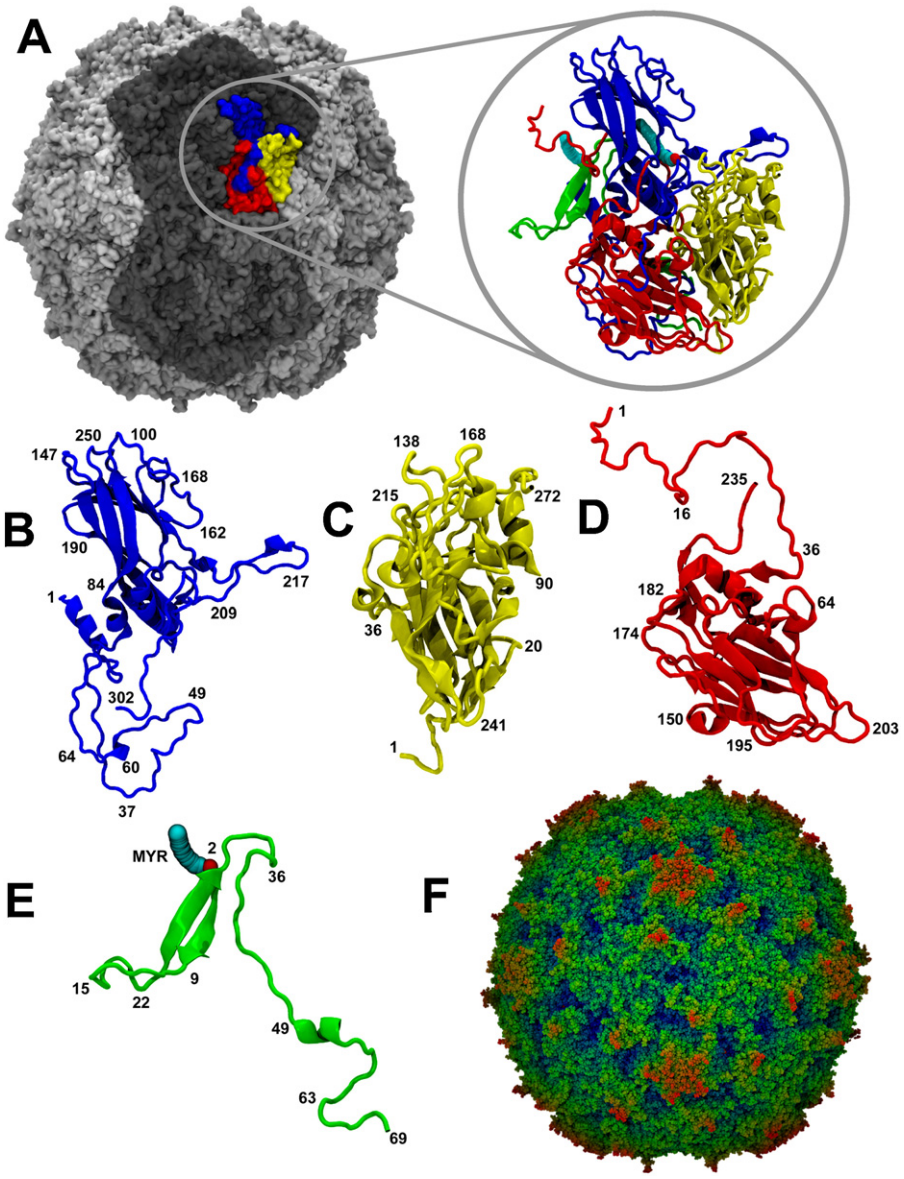

Fig. 1. Structural features of poliovirus. (A) Coloured section shows the relative positioning of a single protomer (1 of 60) within the icosahedral virus capsid. Dark grey shading indicates the relative position of pentamers intersecting at the 2-fold axis of symmetry. The breakout image on the right of (A) shows a cartoon representation of a protomer coloured by chain [26]. (B–E) Individual protomer subunits with selective amino acid residues numbered (B) VP1 = blue, (C) VP2 = yellow, (D) VP3 = red, (E) VP4 = green. (F) All-atom Van der Waals representation of poliovirus virion with radial colouring depicting the relative distance from the centre of the particle with blue = 120 Å to red = 150 Å.

acid sequence of the N-terminus of VP1 in many enteroviruses, including poliovirus and rhinoviruses, reveals a periodicity of hydrophobic residues that may form an amphipathic helix with polar residues along one half of the surface and non-polar residues on the opposite surface [5]. The complete VP1 crystal structure of human rhinovirus 16 was resolved as an amphipathic helix formation at the N-terminus providing support for this structure in other enteroviruses [6].

The N-terminus of VP1 is reversibly exposed to the exterior of native virus particles that sediment at 160S and is capable of binding liposomes, which is believed to be an intermediate step of the cell entry process of poliovirus infection [7,8]. Binding of the poliovirus receptor, CD155, leads to the irreversible externalization of the N-terminus of VP1 and loss of VP4 forming the 135S virus particle [9,10]. The intimate involvement of the N-terminus of VP1 in the poliovirus infection cycle necessitate resolving its structure within the inner surface of the native capsid to gain a better understanding of the molecular processes involved.

The computational power available from supercomputers now enables molecular dynamics (MD) simulations of multi-million atom systems, facilitating the *in silico* investigation of macromolecular structures including viruses [11]. We have utilised MD software to perform atomistic simulations of the complete wild poliovirus type 1 Mahoney strain, including the native RNA sequence, which equated to approximately four million atoms. The X-ray crystallographic co-ordinates of wild poliovirus type1 published in 2001 [12] were used to reconstruct the molecular structure and the missing VP polypeptide sequences were reconstituted according to the published prototype nucleic acid sequence (GenBank NC002058). Given the reported involvement of the N-terminus of VP1 in cellular infection by poliovirus we

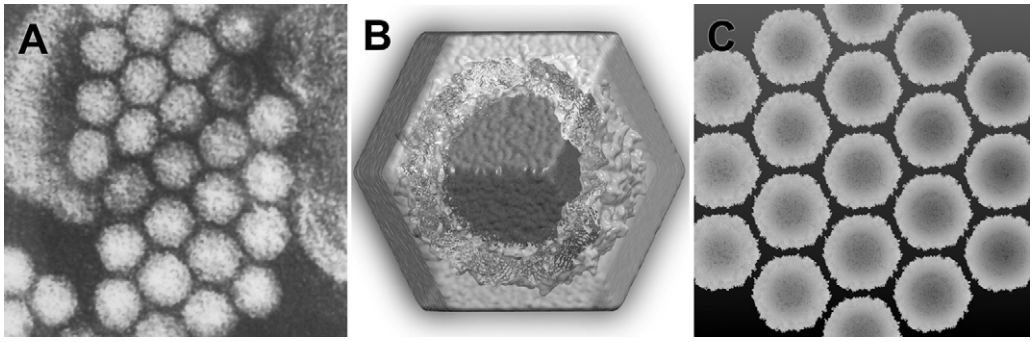

Fig. 2. (A) Transmission electron micrograph of a picornavirus sample showing honeycomb-like aggregation of virus particles. (B) MD simulation of full poliovirus virion suspended in saline solution with transparent density representation of water used to show periodic cell boundaries. (C) Transverse section of periodic cell reflections indicating the similar "honeycomb-like" appearance of the MD simulation of a full poliovirus virion to electron microscopy data.

report an investigation of the proposed amphipathic α-helical structure under various conditions to better understand its intrinsic stability.

2. Methods

Poliovirus capsid reconstructions were based on GenBank sequence ID NC002058. PSIpred predictions [13] derived from the amino acid sequence data and comparative information determined from enterovirus crystal structures available in the Research Collaboratory for Structural Bioinformatics protein data bank (RCSB PDB) were used to select an appropriate template for the reconstruction of the capsid and associated lipids. X-ray crystal structure of poliovirus type 1 Mahoney strain (PDB file 1HXS) at a 2.2 Å resolution [12] was selected as the template.

Reconstruction of the virus was achieved using the Visual Molecular Dynamics (VMD) [14] software package incorporating Compute Unified Device Architecture extensions [15]. A significant element lacking from the original crystal structure was the amino terminus of the VP1 protein common to members of the genus *Enterovirus* and reported to have an α-helical structure [5]. The 19 missing residues constituting the region containing the α-helix were reconstructed using the molefacture plug-in in VMD. Spatial alignment of the helix was based on the positioning of partial coordinate data in the original 1HXS PDB file. Topology files and CHARMM parameter data for the associated myristate and palmitate molecules were determined using the SWISSparam server (http://swissparam.ch/) [16].

Icosahedral symmetry data required to reconstruct the 60 virus protomers into a full capsid structure were available in the form of metadata within the original crystal structure. Using the "mono2poly" tcl script (http://www.ks.uiuc.edu/Research/vmd/script_library/scripts/mono2poly/) a single protomer was positioned according to the biological parameters in order to assemble the 240 proteins and 120 lipids required for a full poliovirus capsid.

In order to recreate a structure analogous to a full wild poliovirus virion, the encoding genomic RNA from GenBank sequence ID NC002058 was spilt into 10 fragments of approximately 750 bp each and the 3′NTR was polyadenylated ($n = 20$). The VPg protein was replicated using the PDB file 2BBP and covalently attached to the 5′NTR of the genome. Each RNA of the 10 RNA fragments was generated in a helical structure approximately 200 nm in length using the "make-na" server (http://structure.usc.edu/make-na/index.html). Steered molecular dynamics was used to compress each fragment to 300 nm. Once compressed the fragments were arranged in a supercoil formation. Steered molecular dynamics was used to direct the super coiled RNA into a sphere approximately 300 Å in diameter then solvated and neutralised in a magnesium chloride solution. The RNA was steered further to 187 Å diameter and encapsidated by the previously constructed poliovirus capsid resulting in a final structure totalling 1.05 million atoms.

An additional 3 million atoms were required to replicate a 0.154 mM sodium chloride solution with cell edge padding at 16 Å on each axis with cubic cell dimensions of 344.8 Å. Due to the inefficient nature of a cubic system for the simulation of an icosahedral structure, rhombic-dodecahedron periodic boundary conditions were chosen to reduce the amount of water required to solvate the virus and better replicate the *in vitro* aggregation of multiple picornavirus particles (Fig. 2).

MD simulation was performed using supercomputers at the Victorian Life-Sciences Computation Initiative (VLSCI) and the Nanoscale Molecular Dynamics (NAMD) software package [17] (http://www.ks.uiuc.edu/Research/namd/). Initially, 50,000 steps of energy minimisation were performed. This was followed by equilibration using a constant particle number, pressure and temperature ensemble (NPT) for 0.5 ns to 310 °K at 1013.25 mbar (one atmosphere) using 256 cores of an SGI Altrix XE supercomputer.

Table 1
Table outlining specific details of each simulation including periodic boundary conditions (PBC) and total atoms used.

Simulation	Detached helix	Pentamer	Empty capsid	Complete virion
Total atoms	8586	388,521	3,938,950	2,754,142
PBC	Cubic	Cubic	Cubic	Rhombic dodecahedron
Amino acids	20	4390	52,680	52,680
Nucleotides (RNA)	0	0	0	7640
Fatty acids	0	10	120	120
Water molecules	2760	106,629	1,038,857	563,929
Sodium ions	10	370	3728	2581
Magnesium ions	0	0	0	3155
Chloride ions	8	309	3011	1607

Once equilibrated the virus simulation was moved to a BlueGene/P supercomputer running NAMD 2.8 beta 1 with memory optimisation extensions on 2048 cores. NPT simulations of a detached α-helix (8586 atoms), pentamer (388,521 atoms), empty capsid (3.94 million atoms) and full virion (2.75 million atoms) were run for 10 ns each (Table 1). Trajectory data for each simulation were then analysed on local computers for structural changes including root mean square deviations (RMSD) and ion permeation (refer to supplementary Fig. 1).

The fit-averaged structure of VP1 within a MD simulation of a pentamer, empty capsid and full virion were compared to the following PDB coordinate files of wild poliovirus type 1 crystal structures: 1HXS, 1AL2, 1AR6, 1AR7, 1AR8, 1AR9, 1ASJ, 1PO1, 1PO2, 1POV, 1VBD.

3. Results

Initial *in silico* reconstructions of the solvated poliovirus virions were in the order of four million atoms using cuboidal periodic boundary conditions (PBC). The adoption of a rhombic-dodecahedral PBC allowed the atom count to be reduced to 2.75 million atoms with a simulation time of 0.79 days/ns (1.27 ns/day) when using 2048 cores of a BlueGene/P supercomputer. After 10 ns of simulation each of the four models (detached α-helix, pentamer, empty capsid and full virion) were transferred locally for analysis.

The full virion structure after 10 ns of MD simulation is shown in Fig. 3. In order to quantify the stability of the simulations, the root mean square deviation (RMSD) values for α-carbons were calculated for pentamer, empty capsid and the full virion (Fig. 4) with a modest increase in RMSD indicating the simulations were stable.

The full virion required more time to stabilise compared to the empty capsid. This was evidenced also by the variation in radius of the two different capsids over the course of the 10 ns simulations (Fig. 5). The empty capsid showed no more than 2% deviation in radius compared to the full virion, which showed an initial increase in radius up until 6.5 ns at which point the virus stabilised. The final virion diameter was approximately 29.5 nm which is consistent with the observed properties of poliovirus virions *in vitro* with a diameter of approximately 30 nm [1] (Fig. 2).

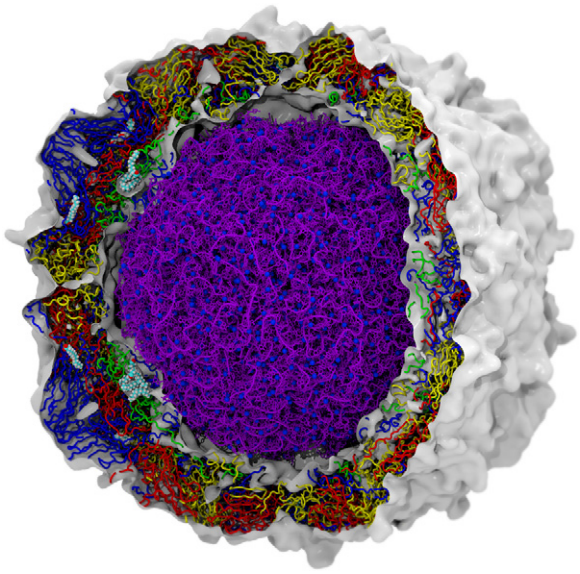

Fig. 3. Poliovirus type 1 (Mahoney strain) after 10 ns of atomistic MD simulation. Total simulation size approximately 2.8 million atoms. Water and surrounding ions have been removed from this representation. Volumetric (density) map representation is represented (white) with protein backbone shown as tubes and coloured by subunit VP1 = Blue, VP2 = Yellow, VP3 = Red, VP4 = Green. Lipids are represented as Van der Waals models with colouring by name of element. RNA is shown using a "liquorice" representation (purple) with associated magnesium ions (Blue).

We also examined the stability of VP1-4 and compared their regions of flexibility with temperature factors from known crystal structures. At the 10 ns time point, each of the 60 individual protomers constituting the virus capsid were transposed to the initial protomer coordinates as defined by the 1HXS template crystal structure. The 60 protomers now occupying the same space were then averaged to give a single "fit-averaged" structure.

The individual fit averaged protomer structures for the pentamer, empty capsid and full virion were compared to the original template coordinates and deviation from the original structure for the VP1 protein was calculated using the RMSD method. RMSD values ranged from 0.873 to 1.099 when compared to the original 1HXS crystal template structure and from

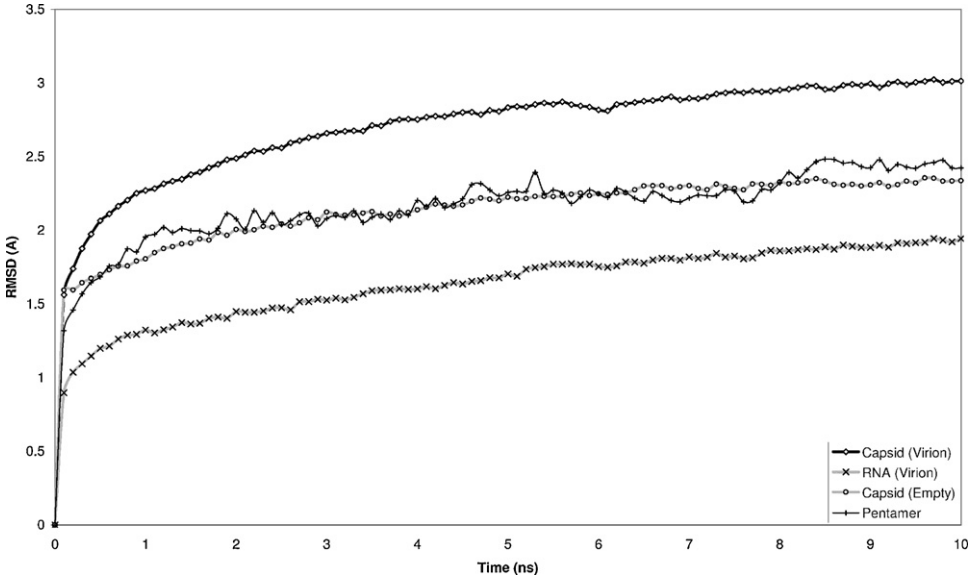

Fig. 4. Root Mean Square Deviation (RMSD) of the poliovirus empty capsid, full virion, spherical RNA alone and an individual pentamer over the 10 ns simulation time.

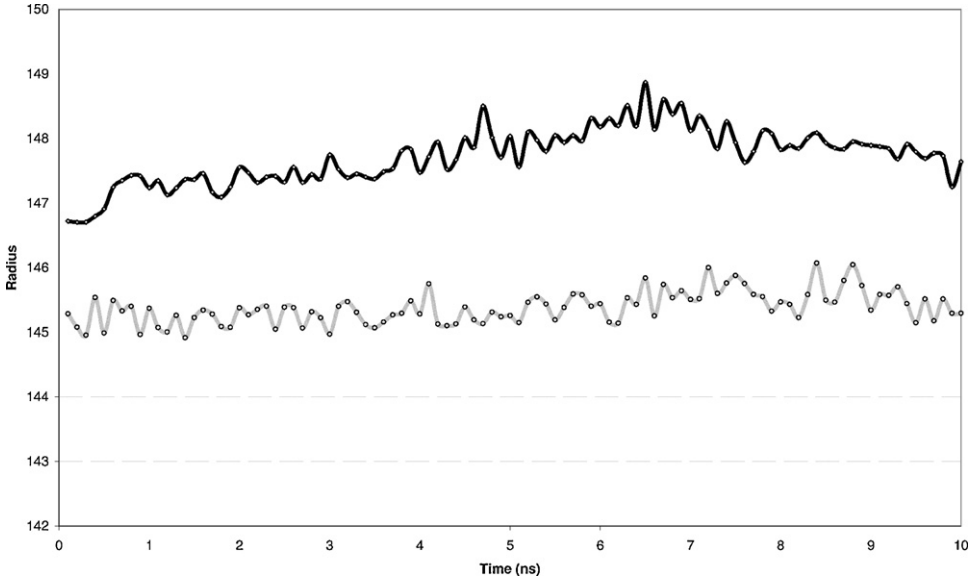

Fig. 5. Average capsid radius (Å) over 10 ns simulation time for empty capsid (grey) and full virion (black).

1.125 to 1.604 for the ten other crystal structures listed in the Methods that were available in the RCSB PDB for comparison (Fig. 6)

Root mean square fluctuation (RMSF) values were calculated for each residue of the 60 protomers for the period 7.5 ns to 10 ns. The average RMSF for each residue was then applied to a fit averaged protomer structure (Fig. 7). This method indicated the relative flexibility of individual amino acid residues. The empty capsid protomers showed significantly increased flexibility in the VP1 N-terminal α-helix and surrounding structures when compared to the full virion (Fig. 7).

The individual amino acids of the capsid proteins were analysed for their proximity to the genomic RNA. The RNA interactions were predominately confined to the amino termini of the capsid proteins VP1, VP2 and VP4 with the exception of a single instance (1 of 60) of residues VP1-267R, VP2-256M and VP2-257C (Fig. 8).

Using the protomer-fit averaging method described above, all 60 protomers were overlayed according to the original 1HXS crystal coordinate file and observed relative to the genomic RNA molecule (Fig. 9). It was noted that the N-terminal α-helix was in close contact with the RNA and partially concealed within the surface of the RNA.

The region obscured by the RNA showed a strong correlation to data missing from the 11 available poliovirus type 1 crystal structures. Two other regions highlighted in Fig. 9, the C-terminus of VP3 and the N-terminus of VP2, which were also missing from the available crystal structures, displayed high RMSD values using the protomer-fit averaging method at the 10 ns time point (Fig. 10).

When comparing the RMSD values of the VP1 protein, particularly with respect to the original 1HXS template structure, it was shown that the α-helix displays higher RMSD values in the empty capsid than that of the full virion (Fig. 11). This is consistent with the α-helix in the empty capsid having increased molecular flexibility when RNA is not in close proximity.

The stability of the putative α-helix of the VP1 N-terminus was analysed in isolation from the remainder of the capsid structure. The detached amino acids (residues one to 20 of VP1) maintained a helical structure for the duration of the 10 ns simulation (Fig. 12a). Significant stabilising elements of this helix are salt bridges between residues ARG15-ASP11 and ARG15-GLU16 (Fig. 12b and supplementary Figs. 2–5). The distribution of amino acid residue types is indicative of an α-helix that is amphipathic by nature and matches previous descriptions (Fig. 12c) [6].

Positive ions, specifically sodium ions, were observed entering the virus core of the full virion and chloride ions were noted leaving the virus core predominately *via* small fissures that formed at the 2-fold axis of symmetry over the 10 ns MD simulation (supplementary Fig. 1). Fissures at the 2-fold axis of symmetry recently have been shown using cryo-electron microscopy to be involved in

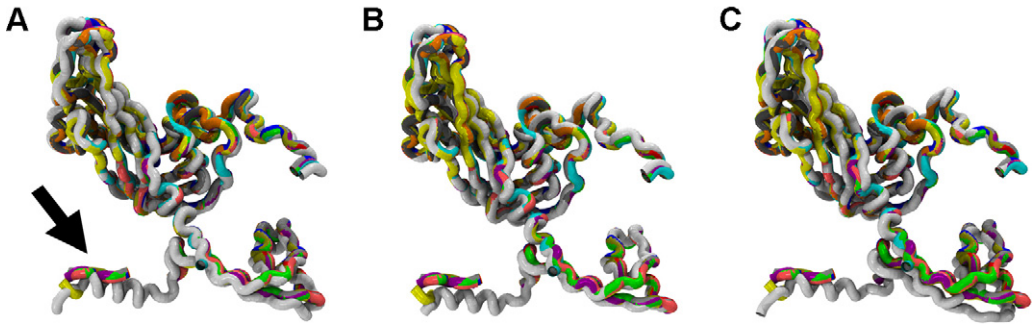

Fig. 6. View of fit-averaged VP1 structural protein (White) overlayed on ten available poliovirus type 1 crystal structure coordinates (coloured) and the original template crystal structure 1HXS (blue) from the RCSB PDB. Arrow indicates the position of the reconstructed amphipathic α-helix after 10 ns simulation of (A) pentamer ($n = 5$), (B) empty capsid ($n = 60$) and (C) full virion ($n = 60$). (For interpretation of the references to color in this figure legend, the reader is referred to the web version of the article.)

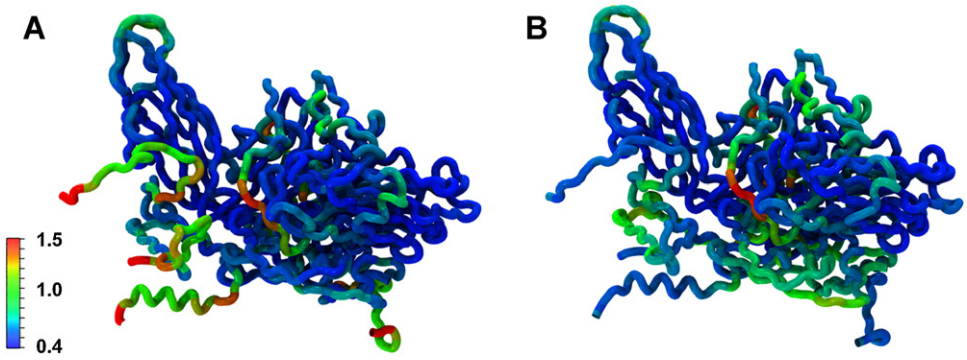

Fig. 7. Root mean square fluctuation RMSF values calculated over 7.5 to 10 ns time period for all protomers *in situ* (A) empty capsid and (B) full virion.

the release of RNA in response to heat treatment [18,19]. Magnesium ions within the virus core were not prone to any significant movement and remained intimately associated with the RNA, a phenomenon observed previously in full virus simulations of satellite tobacco mosiac virus [11]. It was observed that ion movement was not limited to the two-fold axis of symmetry but also occurred *via* a small pore-like structure at the base of the canyon near the entrance to the hydrophobic pocket, this pore-like structure has been observed previously in viruses related to poliovirus such as rhinovirus [20].

4. Discussion

We are investigating MD simulation methodology to build complete human enteroviruses, including the native RNA sequence. We believe that all-atom simulations of enteroviruses will provide insights to significant molecular interactions and biological properties of the virion that cannot be discerned from the modelling of individual structural units or the use of static models. The advantage of full virus simulations is weighed against the increase in the total atom count, which may limit the simulation time. This was addressed by adopting a rhombic dodecahedral formation for the solvated full virus simulation with a one third reduction in the total atom count.

Initially we aimed to validate the atomistic MD simulation of a complete enterovirus by constructing wild poliovirus type 1 (Mahoney strain) and comparing various structural elements with published data. We chose this virus due to the abundance of X-ray crystallography and biochemical analyses published over more than thirty years. We noted that specific regions of the

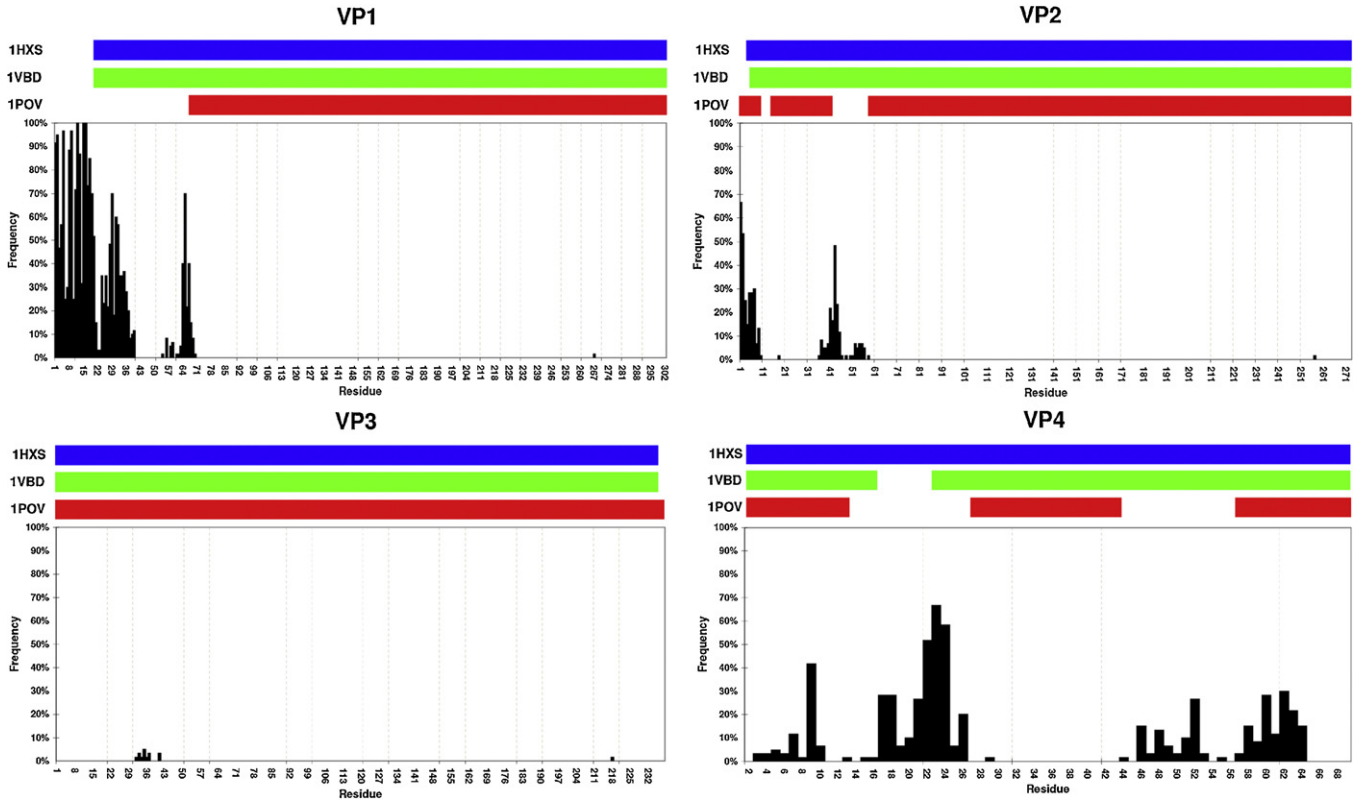

Fig. 8. Bar graph depicting the frequency of amino acids found within a distance of 5 Å from the viral RNA for all 60 capsid protomers. Shaded bars at the top of each chart indicate available coordinate data by residue for the full virion template files 1HXS (blue) and 1VBD (green) and empty capsid 1POV (red). (For interpretation of the references to color in this figure legend, the reader is referred to the web version of the article.)

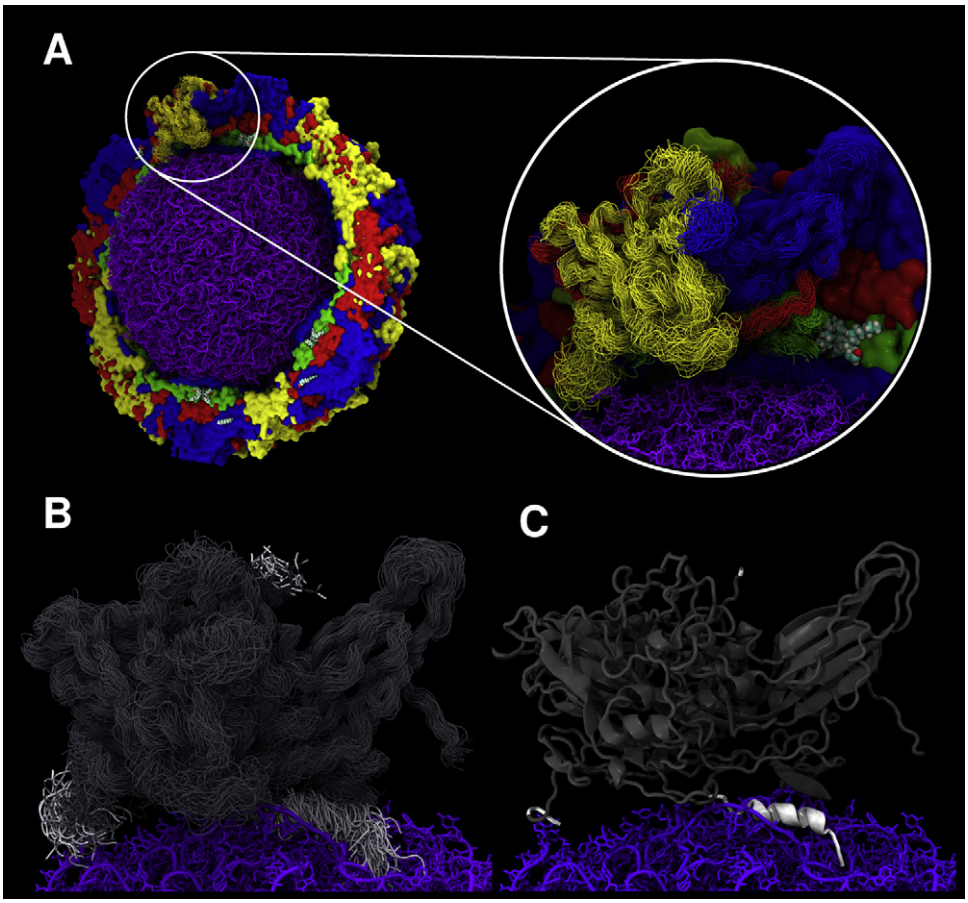

Fig. 9. (A) cutaway representation of the full poliovirus virion highlighting relative positioning of a protomer in relation to the RNA genome (purple). The fit averaged protomer ($n = 60$) is coloured by chain as in previous figures and represented as a backbone structure at the 10 ns time point. (B) Overlaid backbone structure of all 60 fit averaged protomers, structures missing from original X-ray crystal data are highlighted in white. (C) Cartoon representation of the structure derived from the fit averaging procedure. Missing crystal data are highlighted in white.

virus internal structure could not be resolved by X-ray crystallography and wanted to investigate whether this could be due to interaction of the genomic RNA with the capsid proteins by a simulation of the full poliovirus virion. Although the virus capsids display an icosahedral symmetry the structure of underlying genomic RNA has not been determined due to the amorphous nature of the virus core. We thought it important to incorporate the RNA in this structure to better reproduce an infectious particle. An additional advantage of simulating the entire virion is that we also avoid the potential for any simulation artefacts that may arise by simulating a portion of the capsid through symmetry. This could be especially relevant if there is an event that breaks capsid symmetry such as capsid distortion prior to RNA release.

The availability of 60 individual hydrophobic pockets representing 60 independent measurement points will prove useful in terms of statistical and biological relevance for future experiments involving antiviral drug-binding events. The core of the fivefold axis of symmetry displayed variation in flexibility in the presence of RNA when compared to an empty capsid as shown in Fig. 7. It is not known what influence this variation in flexibility would have on the study of drug binding in the hydrophobic pocket. Inclusion of the encoding RNA molecule may also serve to assist researchers studying viral uncoating mechanisms and subsequent RNA release.

The full virus and the individual components (pentamer, empty capsid, spherical RNA) were stable after 10 ns simulation when assessed by RMSD and the average capsid radius of the empty capsid and full virion. The N-terminus of the VP1 protein of poliovirus type 1 has been hypothesised to form an amphipathic α-helix based on the periodicity of the amino acid sequence [5]. The putative amphipathic helical structure was intrinsically stable when the final 20 amino acid residues were simulated as an independent entity, however, a fit averaged structure of the 60 protomer units indicated increased flexibility of the N-terminal region of VP1 when it was part of the empty capsid structure compared to the full virion. At completion of the full virion simulation, the N-terminus of VP1 protruded internally of the capsid in close proximity to the genomic RNA, an orientation that would occlude it from X-ray analysis.

The N-terminus of VP1 is reversibly displayed on the exterior of the virus capsid through virus breathing, a feat that would necessitate molecular flexibility. It was postulated that binding of poliovirus to the cellular receptor, CD155, results in the irreversible externalization of the N-terminus of VP1 as part of cell membrane penetration to form a pore complex for egress of the genomic RNA [5,8]. The orientation of the N-terminus of VP1 on the internal surface of the capsid prior to receptor binding has been the subject of much speculation [5]. The amphipathic helix of the N-terminus of VP1 of human rhinovirus 16 was reported to be located on the interior surface of the capsid along the icosahedral fivefold axis, the orientation described in this study [6]. Recent published data of enterovirus 71 indicated that the positioning of the VP1 α-helix was oriented toward the 2 fold axis of symmetry [21]. In addition, antibodies directed to the poliovirus N-terminus of VP1 were

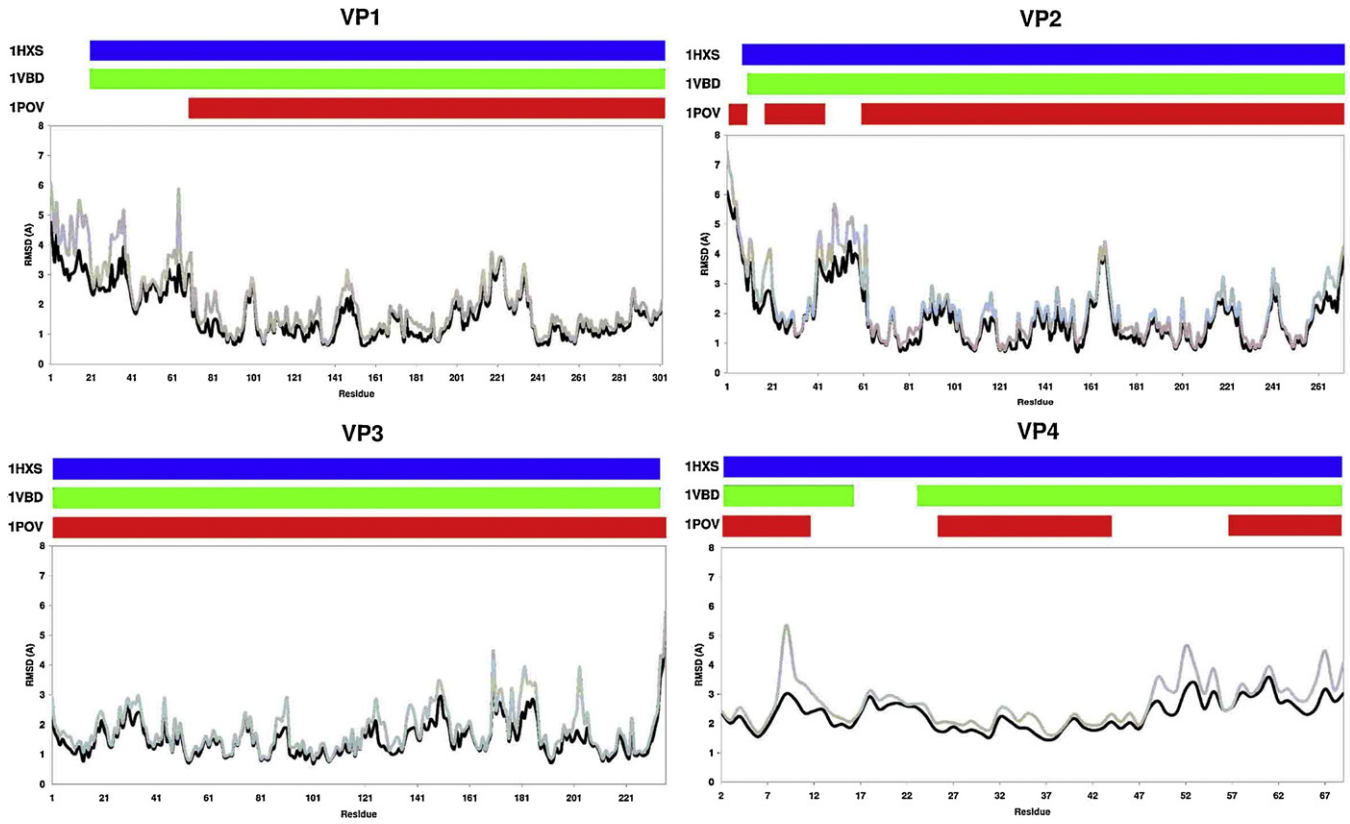

Fig. 10. RMSD of individual residue for fit-averaged protomers ($n = 60$) at the 10 ns time point for empty capsid (grey) and full virion (black). Shaded bars at the top of each chart indicate available coordinate data by residue for the full virion template files 1HXS (blue) and 1VBD (green) and empty capsid 1POV (red). (For interpretation of the references to color in this figure legend, the reader is referred to the web version of the article.)

detected by cryo-EM analysis to be orientated towards the two-fold axis of symmetry [22]. Further studies of this process using the full poliovirus MD model described in this report as a basis will be performed.

Our results show that the detached helix is just as stable as those in full capsids (supplementary Figs. 6–9). The mechanistic implication is that unlike many toxins and viral fusion peptides, the VP1 N-terminal helix may not be required to unfold and refold upon membrane insertion, but rather exists in a pre-formed helix that can readily insert into the membrane [23]. The presence of conserved glycine and proline motifs within the N-terminus of the VP1 protein may act as molecular hinges facilitating the required flexibility for expulsion VP1 during the transition from 160S to 135S conformations [8,24,25].

The production of a stable all-atom MD simulation of wild poliovirus that has been validated against crystallographic data lays the foundation for the modelling of other enteroviruses and picornaviruses or other similar viruses exhibiting icosahedral symmetry. The recent availability of increased computational power should allow significant increases in simulation times approaching microseconds and enhance future simulations involving the repositioning of the VP1 toward the two-fold axis of symmetry and the investigation of RNA models folded using predicted stem loop structures.

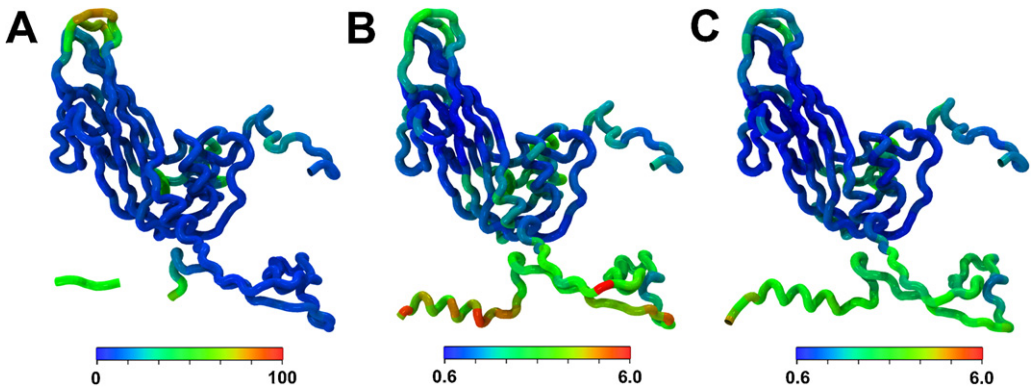

Fig. 11. (A) VP1 protein of the 1HXS template crystal structure coloured by beta value. Figures B and C are coloured "RMSD by residue" of fit averaged VP1 structural proteins ($n = 60$) at 10 ns time point (B) empty capsid and (C) full virion.

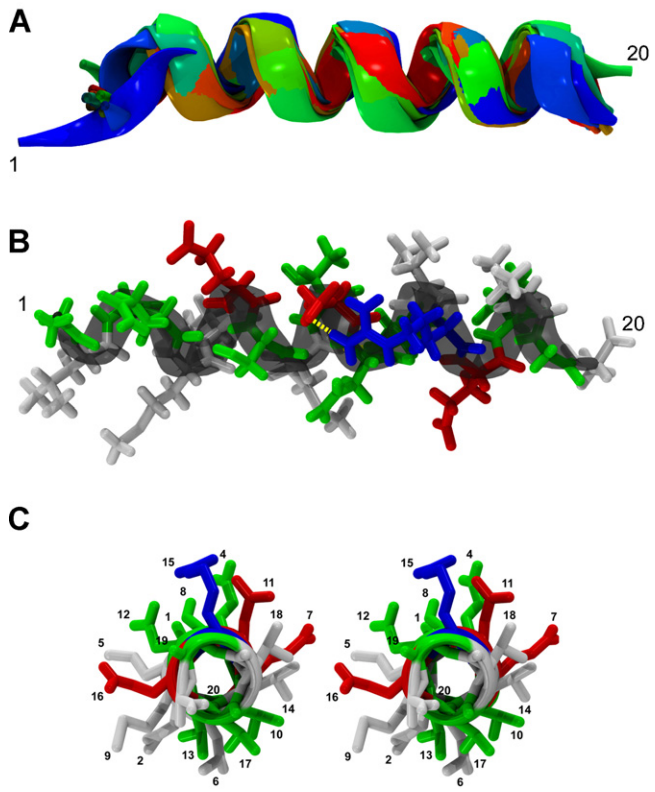

Fig. 12. Detached α-helix from the N-terminus of VP1 after 10 ns simulation. (A) Conformational changes captured at 1 ns time points, (1 ns = blue, 10 ns = red). (B) Liquorice representation of amino acid side chains, showing salt bridge between ARG and ASP (centre), (hydrophobic = white, polar = green, basic = blue, acidic = red, yellow = Hydrogen-bond. (C) Stereo representation of side chain charge distribution around the amphipathic helix.

Acknowledgements

We would like to thank Dallas Wilson, Thomas Aiken and Mike Catton of the Victorian Infectious Diseases Reference Laboratory for supportive contributions at various stages of this work. We thank Cyril Reboul, Grischa Meyer and Matthew Downton for their kind assistance with the generation of the rhombic dodecahedral modelling conditions. We thank the VIDRL Electron Microscopy Unit for their kind provision of the picornavirus transmission electron microscopy image.

We would like to acknowledge and thank nVidia™ for providing access to a Tesla C2070 GPU for the purposes of this study.

This research was supported by a Victorian Life Sciences Computation Initiative (VLSCI) grant number VR0069 on its Peak Computing Facility at the University of Melbourne, an initiative of the Victorian Government, Australia.

The National Enterovirus Laboratory and WHO Regional Poliomyelitis Reference Laboratory are supported by funding from the Victorian State Government, the Department of Health and Ageing, Australia and the World Health Organization.

Appendix A. Supplementary data

Supplementary data associated with this article can be found, in the online version, at http://dx.doi.org/10.1016/j.jmgm.2012.06.009.

References

[1] N.J. Knowles, et al., Family Picornaviridae, in: A.M.Q. King, et al. (Eds.), Virus taxonomy. Ninth report of the International Committee on Taxonomy of Viruses, Academic Press, 2012, pp. 855–880.
[2] J. Hogle, M. Chow, D. Filman, Three-dimensional structure of poliovirus at 2.9 Å resolution, Science 229 (1985) 1358.
[3] R. Basavappa, D. Filman, R. Syed, O. Flore, J. Icenogle, J. Hogle, Role and mechanism of the maturation cleavage of VP0 in poliovirus assembly: structure of the empty capsid assembly intermediate at 2.9 Å resolution, Protein Science 3 (1994) 1651–1669.
[4] D. Baltimore, Picornaviruses are no longer black boxes, Science 229 (1985) 1366.
[5] J.M. Hogle, Poliovirus cell entry: common structural themes in viral cell entry pathways, Annual Review of Microbiology 56 (2002) 677.
[6] A.T. Hadfield, W. Lee, R. Zhao, M.A. Oliveira, I. Minor, R.R. Rueckert, et al., The refined structure of human rhinovirus 16 at 2.15 Å resolution: implications for the viral life cycle, Structure 5 (1997) 427–441.
[7] C.E. Fricks, J.M. Hogle, Cell-induced conformational change in poliovirus: externalization of the amino terminus of VP1 is responsible for liposome binding, Journal of Virology 64 (1990) 1934–1945.
[8] D. Bubeck, D.J. Filman, N. Cheng, A.C. Steven, J.M. Hogle, D.M. Belnap, The structure of the poliovirus 135S cell entry intermediate at 10 Å resolution reveals the location of an externalized polypeptide that binds to membranes, Journal of Virology 79 (2005) 7745–7755.
[9] S. Curry, M. Chow, J.M. Hogle, The poliovirus 135S particle is infectious, Journal of Virology 70 (1996) 7125–7131.
[10] Y. Huang, J.M. Hogle, M. Chow, Is the 135S poliovirus particle an intermediate during cell entry, Journal of Virology 74 (2000) 8757–8761.
[11] P.L. Freddolino, A.S. Arkhipov, S.B. Larson, A. McPherson, K. Schulten, Molecular dynamics simulations of the complete satellite tobacco mosaic virus, Structure 14 (2006) 437–449.
[12] S.T. Miller, J.M. Hogle, D.J. Filman, Ab initio phasing of high-symmetry macromolecular complexes: successful phasing of authentic poliovirus data to 3.0 Å resolution, Journal of Molecular Biology 307 (2001) 499–512.
[13] L.J. McGuffin, K. Bryson, D.T. Jones, The PSIPRED protein structure prediction server, Bioinformatics 16 (2000) 404.
[14] W. Humphrey, A. Dalke, K. Schulten, VMD: visual molecular dynamics, Journal of Molecular Graphics 14 (1996) 33–38.
[15] J.E. Stone, J.C. Phillips, P.L. Freddolino, D.J. Hardy, L.G. Trabuco, et al., Accelerating molecular modeling applications with graphics processors, Journal of Computational Chemistry 28 (2007) 2618–2640.
[16] V. Zoete, M.A. Cuendet, A. Grosdidier, O. Michielin, SwissParam: a fast force field generation tool for small organic molecules, Journal of Computational Chemistry (2011).
[17] J.C. Phillips, R. Braun, W. Wang, J. Gumbart, E. Tajkhorshid, et al., Scalable molecular dynamics with NAMD, Journal of Computational Chemistry 26 (2005) 1781.
[18] H.C. Levy, M. Bostina, D.J. Filman, J.M. Hogle, Catching a virus in the act of RNA release: a novel poliovirus uncoating intermediate characterized by cryo-electron microscopy, Journal of Virology 84 (2010) 4426.
[19] M. Bostina, H. Levy, D.J. Filman, J.M. Hogle, Poliovirus RNA is released from the capsid near a twofold symmetry axis, Journal of Virology 85 (2011) 776.
[20] D. Garriga, A. Pickl-Herk, D. Luque, J. Wruss, J.R. Castón, D. Blaas, et al., Insights into minor group rhinovirus uncoating: the X-ray structure of the HRV2 empty capsid, PLoS Pathogens 8 (2012) e1002473.
[21] X. Wang, W. Peng, J. Ren, Z. Hu, J. Xu, Z. Lou, et al., A sensor-adaptor mechanism for enterovirus uncoating from structures of EV71, Nature Structural & Molecular Biology (2012).
[22] J. Lin, L. Lee, M. Roivainen, D.J. Filman, J.M. Hogle, D.M. Belnap, Structure of the fab-labeled 'Breathing' state of native poliovirus, Journal of Virology (2012).
[23] G.S. Hong, C.P. Chen, M.H. Lin, J. Krüger, C.F.W. Becker, R.H.A. Fink, W.B. Fischer, Molecular dynamics simulations and conductance studies of the interaction of VP1 N-terminus from polio virus and gp41 fusion peptide from HIV-1 with lipid membranes, Molecular Membrane Biology (2012) 1–17.
[24] S.P. Sansom, M. Weinstein, H. Hinges, swivels and switches: the role of prolines in signalling via transmembrane [alpha]-helices, Trends in Pharmacological Sciences 21 (2000) 445–451.
[25] S. Trabulo, A.L. Cardoso, M. Mano, M.C.P. De Lima, Cell-penetrating peptides—mechanisms of cellular uptake and generation of delivery systems, Pharmaceuticals 3 (2010) 961–993.
[26] D. Frishman, P. Argos, Knowledge-based protein secondary structure assignment, Proteins: Structure, Function, and Bioinformatics 23 (1995) 566–579.